A Smart Antenna Receiver Array Using a Single RF Channel and Digital Beamforming

Jonathan D. Fredrick, *Student Member, IEEE*, Yuanxun Wang, *Member, IEEE*, and Tatsuo Itoh, *Fellow, IEEE*

***Abstract*—A new type of smart antenna array receiver with adaptive beamforming is proposed. The novel system offers a drastic reduction in hardware requirements for the smart antenna system through the use of a new Spatial MultIplexing of Local Elements (SMILE) scheme. In this scheme, a single element of the array is sequentially connected to signal processing circuitry in order to sample the incoming modulated carrier. The sampling rate is higher than the signal bandwidth so that the information of the original signal can be fully restored in the post stages using low-pass filters. This system offers an N times reduction in RF hardware for an N-element array. A four-element prototype is built. System principles, SNR, advantages, and hardware, including a new type of array feed network, are discussed. The system performance is validated through a link test with digitally modulated data.**

***Index Terms*—Digital beamforming (DBF), smart antenna, Spatial MultIplexing of Local Elements (SMILE), spatial multiplexing.**

I. Introduction

SMART antennas with digital beamforming (DBF) have revolutionized the capabilities of antenna arrays. Early DBF projects were motivated by military interests, where no-compromise designs were possible at great expense [1], [2]. However, with growing interest in low-cost wireless local area networks (WLANs), the DBF approach is investigated for use in simple high-volume applications where resilience to interference and high user density are desired. The DBF system provides several advantages over analog beamforming techniques. First, analog array systems often use expensive microwave phase shifters and attenuators for each element. Second, the signal processing capability, such as adaptive beamforming of analog systems, is usually limited [3]. For a high throughput system, hybrid analog–digital beamforming techniques have been used to successfully demonstrate adaptive beamforming, adaptive nulling, and improved signal-to-interference ratio [4]–[6]. However, there are still many challenges in the practical implementation of high-performance DBF array systems. First, modern array signal processing is usually performed on the IF or baseband signals. It requires that the signal amplitude and phase information be conveyed properly from the antennas to the post stages or vice versa. Consequently, in conventional array receivers, an independent RF channel is needed for each antenna element. For an N-element array, the total number of RF channels required is N. Therefore, the hardware expense and power consumption of such a system is approximately N times those in a single antenna system. Furthermore, arrays with multiple feed lines and complicated RF circuits introduce more circuit noise and thus are more difficult to integrate into a small area. These are the major hurdles for extensive deployment of smart antenna systems in wireless terminals.

Many efforts have been carried out to reduce the repetitive use of RF hardware in the past. One approach is presented by loading reactive components to each antenna element to control the individual signal phase before combining [7]. The drawback of this approach is that the signal phase and magnitude information is lost after combining, and therefore advanced vector signal processing capability is not possible. In [8], the authors also propose a space-hopping scheme to reduce the number of RF channels to one. However, the approach is based on the alignment of the sliced data symbols into the same bit period. Thus, the application is limited in certain environments since not all of the original signal information is retained. Additionally, the complicated timing control unit and variable delay lines placed at the antennas are hard to realize in practice.

In this paper, we propose a new receiving smart antenna array utilizing a novel Spatial MultIplexing of Local Elements (SMILE) technique in conjunction with DBF. The basic objective of the SMILE approach is to reduce the required number of RF channels to one, without loss of signal fidelity. This is achieved by turning on and off individual antenna elements sequentially at a speed above the signal bandwidth. This is equivalent to sampling the modulated carrier using sequential pulses. The spatially sampled signals from different elements are then multiplexed to form a single feed line output, in a way similar to the time division multiple addressing (TDMA) scheme in communications. Proceeding amplification and down conversion, the signal is demultiplexed at either an IF or to the baseband to recover the original signal from each antenna path. By applying low-pass filters after the demultiplexer, the signals are fully restored without loss of information based on the Nyquist sampling law. Hence, the restored signals from multiple antenna paths can be sampled and processed in the digital domain for beamforming.

The SMILE technique greatly reduces the need for RF hardware. The proposed system achieves the functionality of a fully populated smart antenna system with a fraction of the hardware requirements. Compared to an N-element traditional smart antenna array, the proposed system offers an N-fold reduction in RF hardware requirements. It thus also reduces the power dissipation and circuit size. Due to the reduction in RF

Manuscript received March 14, 2002; revised August 19, 2002.

The authors are with the Electrical Engineering Department and the Microwave Electronics Laboratory, University of California, Los Angeles, CA 90095 USA (e-mail: jfredrick@ieee.org).

Digital Object Identifier 10.1109/TMTT.2002.805150

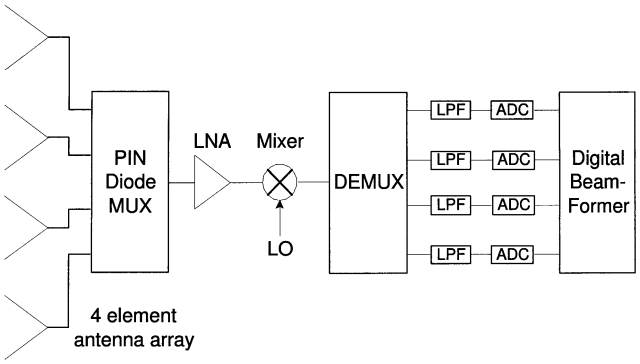

Fig. 1. SMILE system block diagram.

circuit complexity, the use of the SMILE technique will become more prevalent as array dimension and functional requirements increase. However, sampling in a microwave network is challenging since switching among different antenna elements will introduce a change in impedance matching characteristics. Therefore, the feed network for real-time multiplexing has to be designed carefully.

In this paper, the system block diagram is first described along with the operating principals of the system. Receiver SNR, sampling rate, and noise figure performance are then discussed in detail. An antenna array integrated with a p-i-n diode multiplexing feed network is illustrated as a key building block of the system. Measured data are then given to validate the performance of the feed network and multiplexing function. After that, the complete system is placed in a test bed for performance assessment. Measurements are made to verify the SMILE system's ability to maintain the vector signal information of each channel. A DBF algorithm is then used to demonstrate the adaptive beam scan capability of the system. Finally, a simple link test is carried out for digitally modulated data, based on which comparisons between the results with and without DBF are made.

II. System Principles

The block diagram of the SMILE system is shown in Fig. 1. The system consists of an antenna array with an integrated multiplexing network, a digital sequence generator, a single RF channel including low-noise amplifier (LNA), mixer, and analog demultiplexer, low-pass filters, analog-to-digital (A/D) sampling circuitry, and digital signal processor (DSP). The multiplexing network is driven by the digital sequence generator so that the N channels of signal from N antenna elements are sequentially multiplexed to form a single-channel RF output. The switch-driving waveform is shown in Fig. 2. Considering a signal from one of the elements with carrier frequency f_c and modulation bandwidth B, the multiplexing acts as a sampling process with rectangular pulses. The shape of the power spectrum due to the sampling is illustrated in Fig. 3(a), which is a repetition of the modulation spectrum centered at the carrier frequency. The envelope of the repetition follows a $\mathrm{sinc}(x)^2$ and the width of the main lobe of the envelope is $2/\tau_s$. These parameters are determined from the Fourier transform

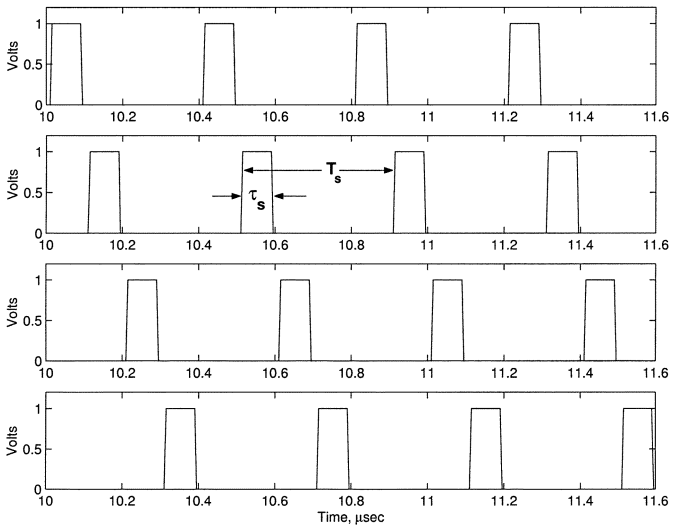

Fig. 2. Digital sequence switch timing diagram.

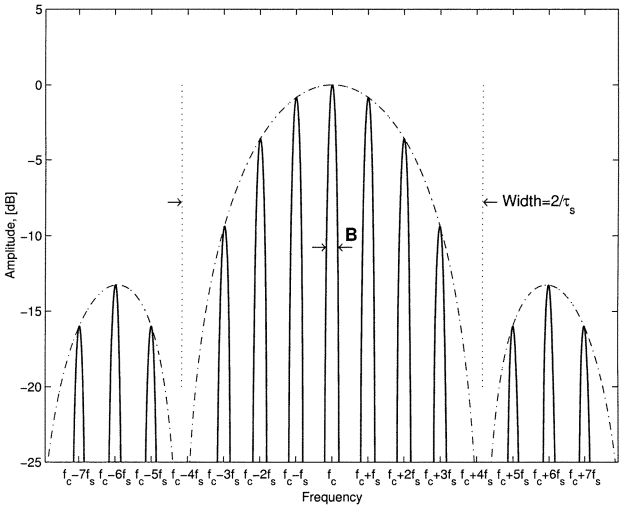

(a)

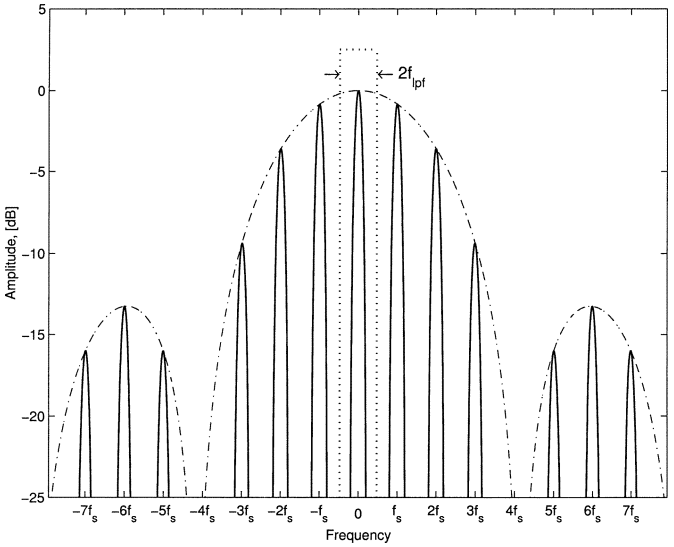

(b)

Fig. 3. (a) Modulated carrier and sidebands. (b) Baseband spectrums with low-pass filter.

of a sampling pulse of width τ_s. The spacing between repeated spectra is due to periodic sampling at $f_s = 1/T_s$. For an array with N elements, $f_s = 1/T_s = 1/N\tau_s$. To avoid the aliasing effects (overlapping of the modulation spectrum), the minimum switching rate is determined by the Nyquist sampling theory, which is given by

$$f_s = B \times N. \tag{1}$$

Therefore, the signal bandwidth received by this system is also limited by the switching speed of the device.

After the multiplexing, the single-channel RF output is amplified and down converted to baseband or an IF depending upon mixer configuration. The analog demultiplexer, driven by the same sequence generator, is then used to separate the signal from different channels. Assuming a zero IF frequency, the down converted signal has a shifted spectrum as shown in Fig. 3(b). To restore the original modulation information, a low-pass filter can be used to reconstruct the continuous signal from the samples. The cutoff frequency $f_{\rm lpf}$ of the filters is selected to allow the basic modulation frequency components to pass. It should be

$$B/2 < f_{\rm lpf} < f_s - B/2. \tag{2}$$

The passband of the low-pass filter is outlined in Fig. 3(b). The signal is then digitized by the analog/digital converters (ADCs). The beamforming is carried out in digital domain. If the system is configured as a heterodyne down converter, then a bandpass filter is needed and the final conversion to baseband may be done in the digital domain. The spectral efficiency of the modulation used must be considered when selecting the sampling rate and filter cutoff. A spectrally inefficient modulation scheme, such as binary phase-shift keying (BPSK) without pulse shaping, will consume more bandwidth in practice than the data rate suggests.

A. SNR

One of the goals of the SMILE system is to achieve the same SNR and interference suppression performance as traditional DBF arrays without the substantial hardware costs. Sampling affects the spectrum of both the received signal and noise. When the envelope of the signal is sampled, the noise and signal spectrums both spread according to the Fourier transform of the sampling function, as illustrated in Fig. 3. The signal and noise are then down converted and passed through the low-pass filters. Assuming that the antenna has a bandwidth matched to the received signal, the in-band SNR has remained constant; however, the in-band signal energy has been reduced by a factor of N^2 compared to that of the conventional array.

A simple analysis of the antenna diversity gain is carried out here. In basic combining techniques, noise in each channel is independent of the signal and is additive [9]. Without considering fading and multipath, the incoming signal from incident angle θ can be represented as

$$r_m = \widetilde{r}_0\, e^{\jmath kdm\cos\theta} \tag{3}$$

and the received noise as $\widetilde{\mathcal{N}}_m$.

Thus, the SNR of the incoming signal at each antenna element is given by

$$\text{SNR}_{\rm single} = \left(\frac{r_m}{\widetilde{\mathcal{N}}_m}\right)^2. \tag{4}$$

For maximum ratio combining, coefficients of equal magnitude

$$a_m = e^{-\jmath kdm\cos\theta} \tag{5}$$

are applied to each channel's signal to achieve the desired radiation pattern. Therefore, the SNR for an N element array is

$$\text{SNR}_{\rm array} = \frac{\left|\sum_{m=1}^{N}\widetilde{r}_m\right|^2}{\sum_{m=1}^{N}\widetilde{\mathcal{N}}_m^2} = \frac{\left(\widetilde{r}_0 N\right)^2}{\widetilde{\mathcal{N}}_m^2 N} = N \times \text{SNR}_{\rm single}. \tag{6}$$

Thus, it is clear that the diversity gain of the SMILE receiver is equivalent to that of a DBF smart antenna.

B. Internal Loss Components and Noise Figure

The above SNR analysis is based on an ideal noiseless receiver assumption. However, due to the design goals of the SMILE receiver, an LNA is not the first component in the signal's path after the antenna element, thus noise figure is of concern. Each channel has approximately 1.3 dB of insertion loss before the LNA, including the p-i-n diode and metal loss. This value contributes directly to the noise figure of the system and therefore puts an added strain on the system LNA. With current process technology, it is fairly common to see LNAs with noise figures below 0.5 dB with more than 20 dB of gain. Since each channel receives $1/N$ of the signal power, the LNA gain requirement is increased by $10\log_{10} N$ to retain comparable signal amplitude at the output of the mixer.

III. Hardware Implementation

A. Antenna Array and Feed Network

A four-element array is used in the current system implementation. The antenna element in this array is the quasi-Yagi antenna proposed in [10]. This antenna element is well suited for array applications, with wide bandwidth, 90° flat pattern, and mutual coupling below -20 dB. A photograph of the array is shown in Fig. 4. The circuit is fabricated on RT/Duroid 6010.2 substrate, $\epsilon_r = 10.2$, with a thickness of 50 ml, and is uniplanar in design. Array element spacing is half a free space wavelength at 5.8 GHz. In the photo, the p-i-n diodes are located just beneath the radial bias stubs of each element. A dc bias return is located near the SMA connector. The switch driver circuit is implemented with 74AC series CMOS logic such as a counter, decoder, and inverters.

The new SMILE technique used in this design necessitates a new type of array feed network. Since array phasing is important, a parallel feed network is integrated with the antenna array. However, as each element is switched on and off, the loading of the antenna to the feed network changes from 50 Ω to an open circuit. A schematic of the feed network used is shown in Fig. 5.

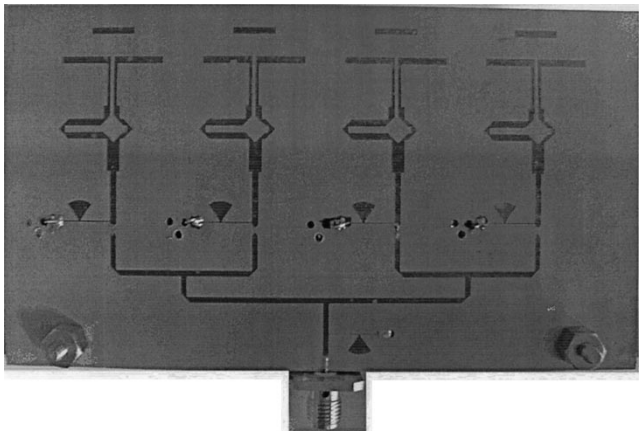

Fig. 4. Photograph of the four-element antenna array with p-i-n diode switches.

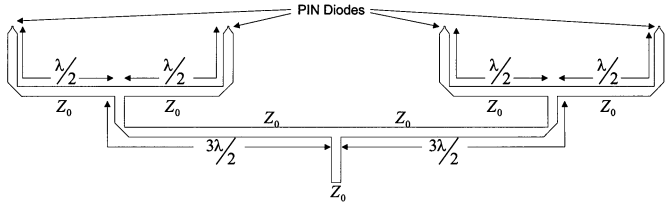

Fig. 5. Schematic of the always matched feed network.

In the figure, the switch reference plane is the location at which the loading change occurs. The T-like junctions shown are not traditional T-junctions. In this case, all three transmission lines have a characteristic impedance of 50 Ω. The network is designed to always be matched to 50 Ω at its input when exactly one antenna element is active. In order to achieve this goal, the length of the feed lines is tuned in order to bring the open circuit impedance presented by the switch to the edge of the transmission line junction. Thus, the open circuit does not load the feed network. By carefully selecting the length of feed lines, it is also possible to minimize the mutual coupling between the array elements since only one element is on each time.

To test the performance of the feed network, a connectorized circuit is assembled with p-i-n diode switches. Each channel is connected to an Agilent 8510C network analyzer. Measured S-parameters of each channel are shown in Fig. 6. Each individual channel has a bandwidth of more than 200 MHz for a voltage standing-wave ratio (VSWR) of less than 2 : 1. The delay of the feed network poses a return loss bandwidth limitation to the system. Thus, for the feed network presented here, a potential symbol rate of approximately 100 Mb/s is allowed. Insertion loss of each channel is approximately 1.7 dB, including 0.4 dB from two SMA connectors and 0.6 dB from the p-i-n diode. The insertion phase of each channel was verified to be equal. The p-i-n diodes used in this design are Agilent Technologies' beam-lead diodes, HPND-4005, and have an off-state (zero dc bias) isolation of 15 dB. Simulations in Agilent ADS indicate that a static phase error results from adjacent channel leakage at 15 dB below the on-state channel. This error varies with the array's deviation from boresite and active element, with several zeros and maxima between 0° and 90°. This error may be compensated for in DSP since it is static in nature. Additional

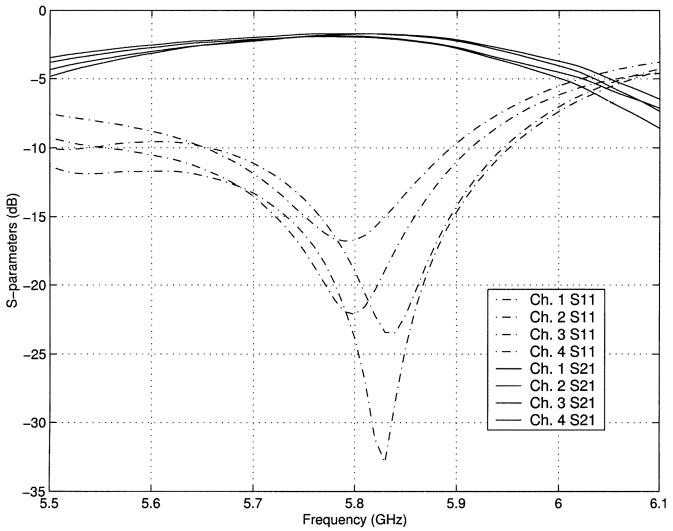

Fig. 6. S-parameters of the feed network, each channel activated sequentially.

isolation is obtainable with reverse bias at the expense of complicating the switch driver circuit.

It should be noted that special care must be taken when switching the p-i-n diodes rapidly with digital pulses due to the large amount of charge stored in the I region of the diode [11]. A residual tail, due to this stored charge, on the falling edge of the pulse will allow the switch to remain on the outside of its time slot. The result of having two switches on at the same time is twofold. Primarily, data may become distorted due to two phases being received in a single time slot. This issue becomes a significant source of error as the sampling speed is increased to accommodate higher bit rates. Secondly, when two antenna elements are switched on simultaneously, the impedance matching discussed earlier is adversely affected. This error manifests itself at all array angles and may be seen in the demultiplexed data as distorted sample edges. However, the error becomes most detrimental when the adjacent sample that is corrupting is nearly out of phase. In this case, the signal energies subtract, thereby reducing the amplitude of a single channel.

A partial solution to this problem is a shunt resistor in parallel with the p-i-n diodes' driver circuit to help drain the charge to ground. A more thorough solution currently being investigated is the use of a low-noise switch such as a high electron-mobility transistor (HEMT) or FET. The transistor's gate terminal, having less capacitance and requiring no dc current, would present an easier load to drive with CMOS logic.

B. Analog Demultiplexer

In order to demultiplex each antenna element's signal, the downconverted signal is passed through an analog demultiplexer. Even though a digital domain implementation of the demultiplexer is possible, the use of an analog demultiplexer further reduces hardware requirements on the ADCs and DSP. In [12], a digital demultiplexer is implemented in MATLAB with a digital sampling oscilloscope acting as an ADC on the multiplexed channel. In the case of a digital demultiplexer, the ADC must have a very high bandwidth to accurately

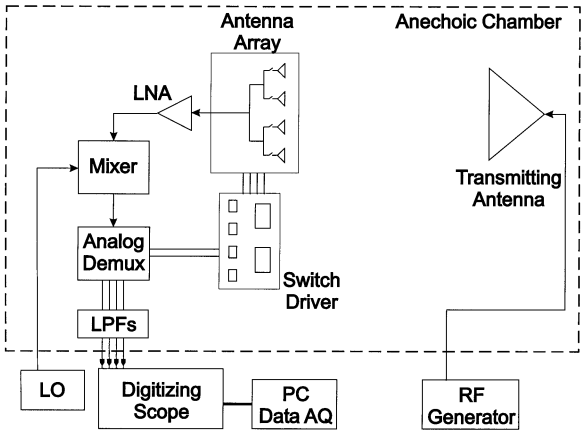

Fig. 7. SMILE receiver testbed setup.

capture the sharp phase discontinuities which occur at large array angles. With an analog demultiplexer, each channel's signal passes through a low-pass filter before being sampled. Therefore, ADC bandwidth is greatly reduced. In this work an Analog Devices ADG-704 4 channel demultiplexer with a 3 dB bandwidth of 200 MHz and negligible loss and dc consumption is used. The ADG-704 operates from the same CMOS counter signal that drives the p-i-n diode switches to ensure low jitter.

IV. Data Recovery and Beamforming Results

A test bed is set up to evaluate system performance. For digital domain processing, a digital sampling oscilloscope is used in place of ADCs and the sampled data is transferred to a PC through a GPIB card for further signal processing in the MATLAB environment. A block diagram of the SMILE receiver test bed is shown in Fig. 7.

A. Single-Tone Test and DBF

A single-tone test was performed first to evaluate the SMILE system's ability to correctly retain array element phasing through sampling and down conversion. The local oscillator (LO) was set at 5.799 25 GHz and RF at 5.8 GHz, providing a 750-kHz IF, thereby eliminating the need for in-phase/quadrature (IQ) demodulators in preliminary tests. Data were recorded at 5° intervals over ±45°. After receiving the signal, each of the four channels of data that were recovered from signal processing are shown in Fig. 8 for the array rotated to +15°, 0°, and −30°. The original data samples are shown along with the envelope. A constant phase front is drawn in each figure to indicate phase progression through the four channels. This test demonstrates the receiver's ability to correctly retain array element phasing through sampling and down conversion. The data in Fig. 8(a) have a smaller amplitude than the other data sets. This error is due to interchannel interference which is caused by the p-i-n diodes not turning off fully before the adjacent channel goes on. This results in contamination of the data in each channel. Certain array angles are more susceptible to this error than others. Other sources of error are physical array position and jitter in the sampling circuit. At angles beyond ±45°, additional signal attenuation occurs due to the antenna elements' directive radiation pattern.

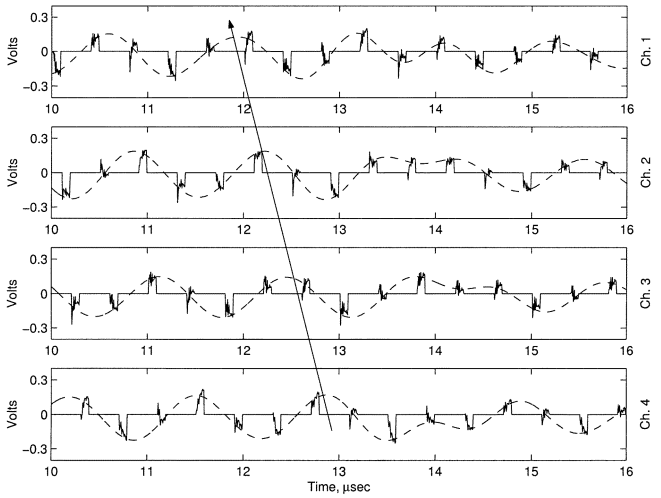

(a)

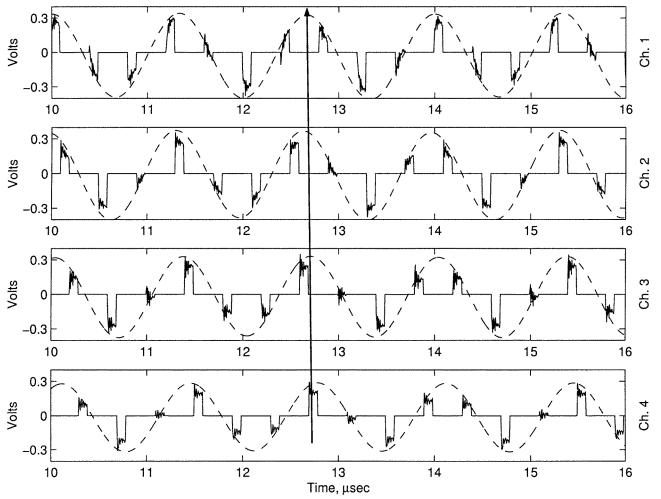

(b)

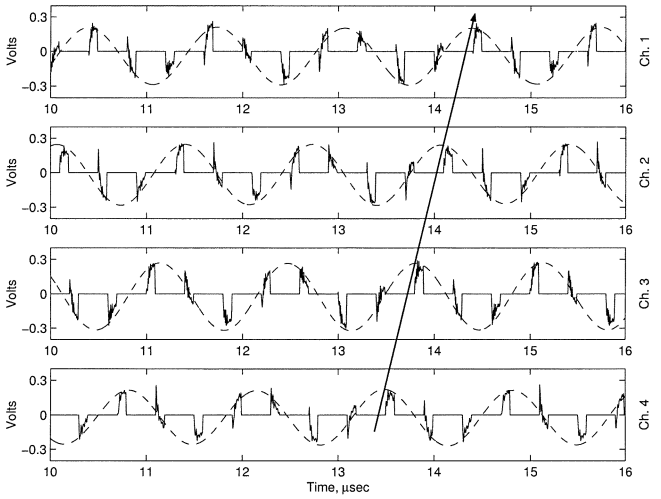

(c)

Fig. 8. Recovered multichannel baseband data for array at: (a) +15°, (b) 0°, and (c) −30°.

Once each channel's data has been recovered, the data are used to form the antenna pattern through the use of DBF. The DBF process allows the antenna's radiation pattern to be

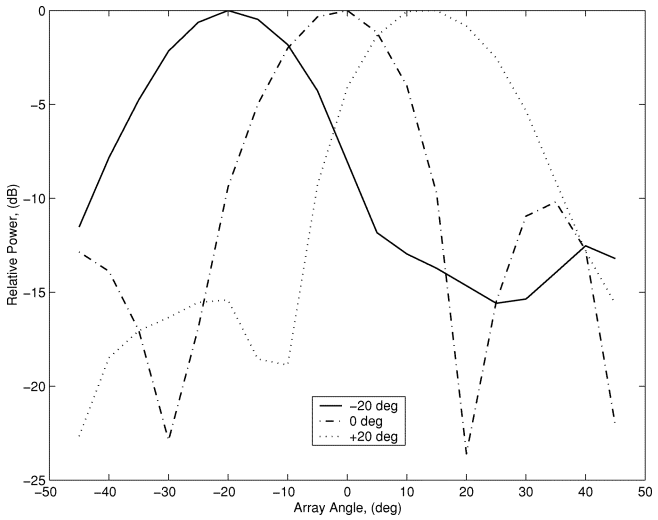

Fig. 9. Baseband DBF radiation pattern.

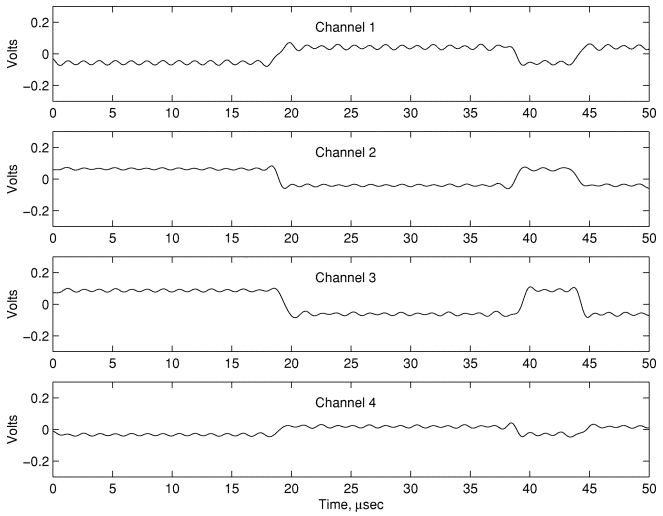

Fig. 10. Each demodulated channel (incoherent) before DBF.

scanned over a wide range of angles without the use of the associated expensive RF hardware. Complex weighting coefficients are multiplied with each channel's data to synthesize the pattern at the desired position. Beamforming results for the new SMILE antenna array are shown in Fig. 9, which plots the beam pattern steered to -20°, 0°, and $+20^\circ$. However, the peak of the antenna pattern for $+20^\circ$ is slightly shifted. As mentioned above, it is due to the asymmetrical phase errors caused by the finite switching speed and leakage of the p-i-n diodes. The antenna can be used for a scan range as far as $\pm 30^\circ$. Beyond that, the edge effects and mutual coupling of the array degrade the antenna pattern.

B. Digital Modulation and Data Recovery

Once the function of the SMILE system was verified with the continuous wave (CW) test, a digital modulation test was performed to verify the system could correctly receive and demodulate digitally modulated data. An RF carrier of 5.8 GHz modulated with a 200-kb/s unfiltered BPSK pseudorandom binary sequence was used to test the SMILE system's ability to receive and correctly demodulate digital signals. The LO was set at 5.799 25 GHz, providing a 750-kHz offset to the RF, thereby eliminating the need for IQ demodulators in preliminary tests. Final demodulation of the data was performed in the MATLAB environment. Higher data rates are achievable by using quadrature mixers and then even further by using faster switching devices.

After the DBF algorithm has been applied, the BPSK data may be demodulated. In order to see the benefits of DBF, the data was demodulated both before and after DBF. In Fig. 10, the array is rotated to -30° and each channel is demodulated individually before DBF. It is clear that, while a binary sequence is visible, the channels have no coherence. In Fig. 11, the unweighted sum of the four demodulated channels (upper frame) is compared to the DBF pattern (lower frame). A significant improvement in signal definition is visible and the binary sequence may be determined with little uncertainty.

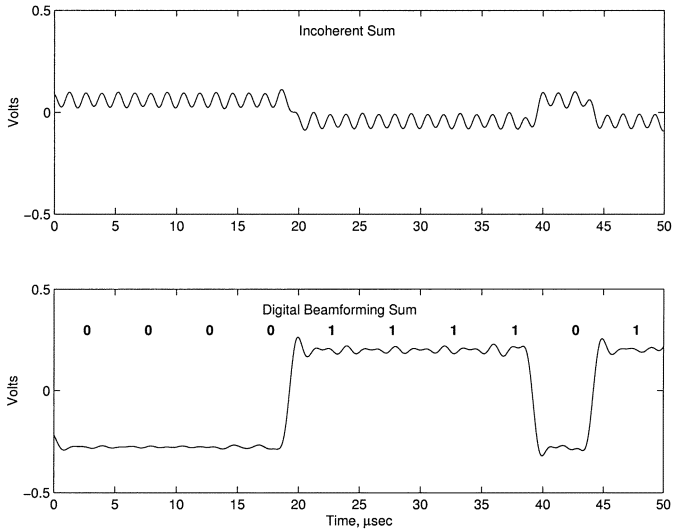

Fig. 11. Recovered digital data, shown before and after DBF.

V. Conclusion

A new type of smart antenna receiver array using a new SMILE scheme, single RF channel, and DBF capabilities has been proposed. This new type of system architecture boasts a significant reduction in RF hardware on board while maintaining plug-and-play compatibility with standard smart antennas. The majority of hardware found on most smart antenna systems, such as analog, RF, and digital, is eliminated through the sampling of the envelope of the received signal at each antenna element. The multiplexed RF signal is then downconverted, demultiplexed, filtered, and then digitized to be processed at lower speeds. The maximum signal bandwidth the system can receive is limited by the sampling rate of the existing switch device and antenna feed network.

A four-element receiver array was prototyped to illustrate the new architecture. The prototype included a new kind of feed network that is always matched during the antenna switching sequence. The performance of the feed network and p-i-n diodes

switches is validated through experiment. It is shown that the SNR and interference suppression is equivalent to a standard smart antenna. Finally, the sampled, downconverted signal is used for DBF in the MATLAB environment and a BPSK modulated carried is successfully demodulated and the DBF algorithms show significant improvement in signal clarity.

ACKNOWLEDGMENT

The authors wish to express their gratitude to S. Jeon, M. Espiau, and the Center for High Frequency Electronics.

REFERENCES

[1] H. Steyskal, "Digital beamforming antennas: An introduction," *Microwave J.*, vol. 30, no. 1, pp. 107–124, Jan. 1987.
[2] H. Steyskal and J. F. Rose, "Digital beamforming for radar systems," *Microwave J.*, vol. 32, no. 1, pp. 121–136, Jan. 1989.
[3] W. Stutzman, J. Reed, C. Dietrich, B. Kim, and D. Sweeney, "Recent results from smart antenna experiments—Base station and handheld terminals," in *Proc. IEEE RAWCON*, 2000, pp. 139–142.
[4] S. Jeon, Y. Wang, Y. Qian, and T. Itoh, "A novel planar array smart antenna system with hybrid analog-digital beamforming," in *IEEE MTT-S Int. Microwave Symp. Dig.*, vol. 1, May 2001, pp. 121–124.
[5] ——, "A novel smart antenna system implementation for broadband wireless communications," *IEEE Trans. Antennas Propagat.*, vol. 50, pp. 600–606, May 2002.
[6] R. Miura, T. Tanaka, I. Chiba, A. Horie, and Y. Karasawa, "Beamforming experiment with a DBF multibeam antenna in a mobile satellite environment," *IEEE Trans. Microwave Theory Tech.*, vol. 45, pp. 707–714, Apr. 1997.
[7] J. Cheng, Y. Kamiya, and T. Ohira, "Adaptive beamforming of ESPAR antenna using sequential perturbation," in *IEEE MTT-S Int. Microwave Symp. Dig.*, vol. 1, May 2001, pp. 133–136.
[8] S. Ishii, A. Hoshikuki, and R. Kohno, "Space hopping scheme under short range Rician multipath fading environment," in *Proc. IEEE Veh. Technol. Conf.*, 2000, pp. 99–104.
[9] V. K. Garg and J. E. Wilkes, *Wireless and Personal Communications Systems*. Upper Saddle River, NJ: Prentice-Hall, 1996.
[10] Y. Qian, W. Dael, N. Kaneda, and T. Itoh, "A uniplanar Quasi-Yagi antenna with wide bandwidth and low mutual coupling characteristics," in *Proc. IEEE AP-S Symp.*, Orlando, FL, July 1999, pp. 924–927.
[11] W. Doherty and R. Joos, *The PIN Diode Circuit Designers' Handbook*. Watertown, MA: Microsemi Corporation, 1998.
[12] J. D. Fredrick, Y. Wang, S. Jeon, and T. Itoh, "A smart antenna receiver array using a single RF channel and digital beamforming," in *IEEE MTT-S Int. Microwave Symp. Dig.*, vol. 1, June 2002, pp. 311–314.

Jonathan D. Fredrick (S'95) was born in Queens, NY, in 1975. He received the B.S. degree in electrical engineering from the State University of New York (SUNY), College at New Paltz, in 1997, and the M.S. and Ph.D. degrees in electrical engineering from the University of California at Los Angeles (UCLA), in 2000 and 2002, respectively.

From 1998 to 2002, he was a Graduate Student Research Assistant with the Electrical Engineering Department, UCLA. His research interests are on the smart antenna receiver arrays and true time delay lines for wireless communications, microwave circuits, integrated circuits, and antennas.

Mr. Fredrick was the recipient of an IEEE Microwave Theory and Techniques Society (IEEE MTT-S) Graduate Student Fellowship in 1999 and 2001, won second place in the Student Paper Competition at the IEEE MTT-S IMS 2002, Seattle, WA, and won first place in the Best Student Paper Competition at the 29th European Microwave Conference, Munich, Germany, in 1999.

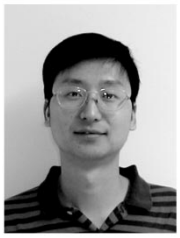

Yuanxun Wang (S'96–M'99) was born in Hubei, China, in 1973. He received the B.S. degree in electrical engineering from the University of Science and Technology of China (USTC), Hefei, China, in 1993, and the M.S. and Ph.D. degrees in electrical engineering from The University of Texas at Austin, in 1996 and 1999, respectively.

From 1995 to 1999, he was a Research Assistant with the Department of Electrical and Computer Engineering, The University of Texas at Austin. Since 1999, he has been with the Department of Electrical Engineering, University of California at Los Angeles (UCLA), where he is currently a Research Engineer and Lecturer. He has authored or coauthored approximately 40 refereed journal and conference papers. His research interests concern the enabling technology for RF and microwave front-ends in wireless communication and radar systems, as well as the numerical modeling, simulation, and feature-extraction techniques for microwave circuits, antennas, and electromagnetic (EM) scattering.

Tatsuo Itoh (S'69–M'69–SM'74–F'82) received the Ph.D. degree in electrical engineering from the University of Illinois at Urbana-Champaign, in 1969.

From September 1966 to April 1976, he was with the Electrical Engineering Department, University of Illinois at Urbana-Champaign. From April 1976 to August 1977, he was a Senior Research Engineer with the Radio Physics Laboratory, SRI International, Menlo Park, CA. From August 1977 to June 1978, he was an Associate Professor at the University of Kentucky, Lexington. In July 1978, he joined the faculty at The University of Texas at Austin, where he became a Professor of electrical engineering in 1981 and Director of the Electrical Engineering Research Laboratory in 1984. During the summer of 1979, he was a Guest Researcher at AEG-Telefunken, Ulm, Germany. In September 1983, he was selected to hold the Hayden Head Centennial Professorship of Engineering at The University of Texas at Austin. In September 1984, he was appointed Associate Chairman for Research and Planning of the Electrical and Computer Engineering Department, The University of Texas at Austin. In January 1991, he joined the University of California at Los Angeles (UCLA), as Professor of electrical engineering and Holder of the TRW Endowed Chair in Microwave and Millimeter Wave Electronics. He was an Honorary Visiting Professor at the Nanjing Institute of Technology, Nanjing, China, and at the Japan Defense Academy. In April 1994, he became an Adjunct Research Officer for the Communications Research Laboratory, Ministry of Post and Telecommunication, Japan. He currently holds a Visiting Professorship at The University of Leeds, Leeds, U.K., and is an External Examiner of the Graduate Program of the City University of Hong Kong. He has authored or coauthored 274 journal publications, 540 refereed conference presentations, and 30 books/book chapters in the area of microwaves, millimeter-waves, antennas and numerical electromagnetics. He has generated 49 Ph.D. students.

Dr. Itoh is a member of the Institute of Electronics and Communication Engineers of Japan and Commissions B and D of USNC/URSI. He became an Honorary Life Member of the IEEE Microwave Theory and Techniques Society (IEEE MTT-S) in 1994. He was the editor-in-chief of the IEEE TRANSACTIONS ON MICROWAVE THEORY AND TECHNIQUES (1983–1985) and the IEEE MICROWAVE AND GUIDED WAVE LETTERS (1991–1994). He serves on the Administrative Committee of the IEEE MTT-S. He was vice president of the IEEE MTT-S in 1989 and president in 1990. He was the chairman of USNC/URSI Commission D (1988–1990), and Chairman of Commission D of the International URSI (1993–1996). He is the chair of the Long Range Planning Committee of URSI. He serves on advisory boards and committees of a number of organizations. He has been the recipient of a number of awards, including the 1998 Shida Award presented by the Japanese Ministry of Post and Telecommunications, the 1998 Japan Microwave Prize, the 2000 IEEE Third Millennium Medal, and the 2000 IEEE MTT-S Distinguished Educator Award.